Nerve-mediated amputation-induced stem cell activation primes distant appendages for future regeneration events in axolotl

Duygu Payzin-Dogru[1]*, Sarah E. Wilson[1]*, Steven J. Blair[1], Burcu Erdogan[1], Shifa Hossain[1], Louis Cammarata[2], Juan Velazquez Matos[1], Alan Wong[1], Julia Losner[1], Sangwon Min[1], Hani Singer[1], Jessica L. Whited[1,3,4]

[1]*Department of Stem Cell and Regenerative Biology, Harvard University, 7 Divinity Avenue, Cambridge, MA, USA, 02138*

[2]*Department of Statistics, Harvard University*

[3]*The Broad Institute*

[4]*The Harvard Stem Cell Institute*

Correspondence: Jessica L. Whited, jessica_whited@harvard.edu

* These authors contributed equally to this work

Summary

Animals exhibit extreme diversity in regenerative ability. This likely reflects different, lineage-specific selective pressures in their evolutionary histories, but how specific molecular features of regenerative programs help solve species-specific challenges has not been examined in detail. Here we discover that, in the highly-regenerative axolotl salamander, a conserved, body-wide stem cell activation response triggered in response to limb removal primes undisturbed limbs for regeneration upon subsequent amputation. This response should be particularly useful to salamanders, which frequently lose limbs in response to cannibalism. We further demonstrate the body-wide response requires both peripheral nervous system input at these distant sites and mTOR signaling. We defined gene expression changes within the nerves and nearby tissues, harboring responsive stem cells, leading to identification of candidate genetic pathways influencing distant stem cell activation following amputation. Functional experimentation confirmed a requirement for adrenergic signaling in amputation-induced activation of distant stem cells. These findings reveal a direct link between systemic cellular activation responses to local tissue damage and overall regenerative ability. Similar systemic activation responses to tissue removal have been observed in animals with widely differing regenerative abilities (e.g., planaria to mice), suggesting that it is the responses downstream of these signals, likely sculpted by differing evolutionary pressures, that ultimately distinguish regenerators from non-regenerators.

Keywords: regeneration, stem cells, axolotl, limb, systemic responses, peripheral nervous system

Main

Loss of a body part provokes cellular and molecular changes at the injury site and systemically [1]. Most research in vertebrate models has focused on local responses, within the remaining "stump" tissues, as cells within these tissues contribute directly to the construction of the new body part. Yet, understanding the mechanism and consequence of systemic responses is critical as they may contribute to regeneration and because comparing them across species may reveal insights related to the evolution of regeneration [2]. The axolotl, a highly-regenerative salamander for which molecular genetic tools now exist [3], provides an extraordinary model for studying regeneration events due to its ability to regenerate complex tissues and organs such as limbs, hearts, and parts of the nervous system. Following amputation in axolotl, a structure essential for regeneration called the blastema forms at the amputation site [4]. The blastema is largely composed of a dense population of highly-proliferative progenitor cells that ultimately undergo differentiation, repatterning, and growth to replace the lost structure. Our current understanding of limb regeneration has focused primarily on local events at the injury site. However, the discovery of a body-wide response to amputation in axolotls [5], in which many distant stem cells are activated to re-enter the cell cycle, raises the possibility that systemic activation may be a component of the regeneration process on which local growth responses are elaborated. Indeed, the activation of stem cells distant from the site of injury is evolutionarily conserved amongst many other species, both super-regenerators (such as planarians) and those with more limited natural regenerative prowess (such as mice) [1, 6-8]. The extensive conservation of this distant-activation phenomenon suggests it is an evolutionarily ancient response and raises the question of whether it is used differently in species with differing regenerative potentials, and, if so, how this relates to specific evolutionary pressures these species face.

Here, we investigate the consequence and mechanism of systemic stem cell activation following amputation in axolotls. We identify potential selective advantages of systemic activation and discover a distant stem cell-priming program driving rapid activation of progenitors and faster proliferation of blastema cells in animals recently challenged with contralateral amputations. Our results highlight mTOR signaling and innervation as critical mediators of systemic activation, with a vital role in the regenerative process. We also use transcriptomics to identify additional candidate signaling pathways controlling systemic activation and implicate adrenergic signaling as a key regulator of systemic activation. Our work reveals the impact evolutionarily conserved systemic cues play in the regenerative process with implications for our broader understanding of the evolution of regenerative competency.

Systemically-activated cells are primed for future regeneration events

We recently reported systemic cell cycle re-entry, defined to be "activation," following limb amputation in axolotl, and identified muscle satellite stem cells to constitute a sizeable fraction of these systemically-active cells [5]. We now demonstrate that among the other cells activated in this system are epidermal stem cells, as defined by their basal position in the tissue and expression of Keratin 10 (K10) (Extended Data Fig. 1). We first reported that systemically-activated cells undergo at least one round of cell division, as evidenced by their expression of phosphorylated Histone H3 [5]. We performed a similar single-pulse EdU experiment, but with a long chase (six weeks). This experiment revealed that systemically-activated cells form small clones, typically 2-4 cells in size (Extended Data Fig. 2), indicating that the response is limited to one or two cell divisions.

To determine if systemic cell activation confers a selective advantage by enhancing the regenerative ability of axolotls, we compared regeneration rates of limbs of systemically-activated animals to those of controls (Fig. 1a). Systemically-activated animals, which received contralateral amputations 7 days prior, exhibited faster blastema growth (blastema area) compared to control animals only receiving a single set of amputations (Fig. 1b, c). The limbs of systemically-activated animals differentiate faster than those of controls, entering the palette stage faster, with outlines of the future digits appearing sooner than in controls, and internal cartilage nodules clearly visible (Fig. 1b, d-e) [9]. Systemic activation of cells in limbs contralateral to an amputation primes them for future regeneration events, enabling the activated limbs to initially coalesce a blastema population of progenitors and then also differentiate them more quickly, ultimately leading to faster regeneration.

mTOR signaling is required for systemic activation

The upregulation of mTOR signaling during regeneration and wound healing is conserved across many species such as planaria, zebrafish, mice, and axolotl [5, 10-13]. In planaria, mTORC1 is necessary for proliferation of neoblast stem cells to promote regeneration [11], and a specific subset of neoblasts characterized as “slow-cycling” during homeostasis relies on mTOR signaling to mount a regenerative response [14]. Furthermore, experimental inhibition of mTOR signaling can counteract hyperproliferation of neoblasts in response to amputation caused by RNAi against *smg1*, a PI3-Kinase-related kinase [10]. Zebrafish caudal fin regeneration also requires mTOR signaling for progenitor cell proliferation, although activation of this pathway in tissues or cells distant to amputation has not been examined in detail [12]. In mice, which repair discrete tissues such as muscle but cannot regenerate full appendages, local tissue injury has been demonstrated to lead to systemic changes as distant stem cells are provoked to enter an “alert“ phase of the cell cycle characterized by increased nuclear size and genome replication [8]. The “alert” state sensitizes distant stem cells to respond more quickly to similar injuries in the future [8]. The conserved activation of mTOR across regenerative models led us to explore mTOR signaling as a requirement for both local and systemic stem cell activation during limb regeneration in axolotl. We sought to answer this question by inhibiting mTORC1 signaling via rapamycin. Rapamycin-treated animals produced smaller blastemas compared to controls (Extended Data Fig. 3). Treatment with rapamycin wholly blocked cell-cycle activation of stem cells systemically in contralateral limbs (Fig. 2a-b). These findings indicate that mTOR signaling is required for stem cell activation at both the local injury site, as well as at distant locations.

Overlap of cells engaging in mTOR signaling and those actively proliferating in systemically activated limbs is scarce [5], implying that non-cell-autonomous effects may control mTOR mediated activation of stem cells at locations distant to the site of injury. In an attempt to identify the conduit transmitting the essential non-cell-autonomous mTOR signal throughout the axolotl body, we examined mTOR activation elsewhere in systemically-activated animals. We analyzed the brains of systemically-activated axolotls, and found robust overlap between expression of phosphorylated s6 Kinase (pS6), a marker for mTOR activation, and NeuN, a marker post-mitotic neurons [15], within the ipsilateral anterior telencephalon, suggesting significant mTOR activation in this region of the brain (Extended Data Fig. 4), and prompting us to explore the nervous system more generally. We examined mTOR activation in potential neuronal processes upstream and downstream of the brain, with relation to limb, such as local peripheral nervous system ganglia. We found that the dorsal root ganglia, which contain the cell bodies of peripheral sensory nerves, are positive for pS6 signal in homeostasis, and that signal intensity

120 increases specifically in the DRG serving the amputated limb (Extended Data Fig. 5). These data imply
121 peripheral nerves may be important for the mediating systemic responses.

122 **Nerves drive systemic activation**

123 Nerve input in the stumps of amputated limbs is an essential requirement for limb regeneration
124 in axolotl and newt [16, 17]. It is also a critical local input in other regenerative contexts in many species,
125 such as heart regeneration in zebrafish and neonatal mice [18]. Recently, the nervous system has been
126 shown to mobilize several stem cell niches in mammalian systems [19, 20]. The upregulation of mTOR
127 signaling in both the central and peripheral nervous systems of systemically activated animals led us to
128 hypothesize that nerves may be the potential agent communicating systemic cues and signals across the
129 body of the axolotl post-amputation (Extended Data Fig. 4 and 5). To test this hypothesis, we transected
130 nerve bundles innervating limbs contralateral to amputations and assayed for successful systemic
131 activation in denervated and sham-operated states (Fig. 3a). Nerve transections performed in intact
132 animals did not induce systemic cell cycle re-entry (Fig. 3b-c). Denervation of limbs contralateral to
133 amputations completely impeded the activation of cells in those appendages demonstrating limb
134 innervation is a requirement in appendages for systemic activation (Fig. 3b-c),

135 Using cell and tissue morphology and location, we classified responding tissues in sham and
136 denervated contralateral limbs to examine the relationship between innervation and cell-type-specific
137 activation. Tissues were classified into three categories: epidermis, skeletal elements, and other internal
138 tissues. Skeletal and internal soft tissues in sham amputated animals displayed a significant increase in
139 EdU+ nuclei compared to intact controls (Fig. 3d-f). Denervated limbs in both intact and amputated
140 states did not exhibit an increase in EdU+ nuclei compared to unamputated controls (Fig. 3d-f). Our
141 results suggest that nerve-mediated systemic activation of distant progenitors is not tissue type specific,
142 indicating peripheral nervous system input is likely required for systemic activation of all limb tissue
143 types in axolotl.

144 **Transcriptomic analyses reveal pathways mediating systemic activation**

145 We next sought to identify candidate factors regulating nerve-mediated systemic cell activation.
146 We performed bulk-tissue RNA sequencing on peripheral nerves, excluding cell bodies, and surrounding
147 tissues in the contralateral limbs of denervated and sham-operated regenerating animals (Fig. 4a). We
148 uncovered 273 differentially-expressed transcripts between intact and transected nerves, and 82
149 differentially-expressed transcripts between activated and unactivated surrounding tissue samples
150 (Supplementary File 1). Our RNA-seq analysis uncovered many genes with known roles in regeneration
151 and cell proliferation, both in axolotl and other regeneration models. Among the transcripts upregulated
152 in transected nerve ends, we identified hepatocyte growth factor (Hgf), a systemic factor shown to
153 stimulate quiescent distant tissue stem cells [8, 21] and transcripts encoding kazal-type serine protease
154 inhibitor 2 (Kazald2) and von Willebrand factor D and EGF domains (VWDE), both of which are blastema
155 cell markers required for axolotl limb regeneration [22, 23]. In surrounding tissue samples of
156 systemically activated animals, we discovered transcripts encoding PCNA (proliferating cell nuclear
157 antigen) to be more highly expressed compared to denervated limbs in which systemic activation was
158 blocked. Conversely, we found downregulation of transcripts encoding serine/threonine-protein kinase
159 Lats1. Inhibition of Lats1, a negative regulator of YAP1 in the Hippo signaling pathway, promotes
160 proliferation in murine cardiomyocytes and also cells in the inner ear [24].

161 We then directed our attention to candidate pathways controlling distant cell activation which
162 have not been extensively studied in the context of limb regeneration. We prioritized investigating
163 transcripts of genes known to encode proteins in signaling pathways, with established chemical
164 inhibitors, for further functional study. Among these candidates was α-2A adrenergic receptor (Adra2a),
165 with transcripts 7.4-fold upregulated in transected nerve ends compared to controls. Adra2a activates
166 hepatic stellate cells in mouse hepatocellular carcinoma models [25] and its silencing has been shown to
167 increase cell proliferation in cervical cancer cell lines through inhibition of the PI3K/AKT/mTOR pathway
168 [26]. We explored the potential role of this gene in systemic cell cycle re-entry by inhibiting the function
169 of its encoded protein with yohimbine, a well-studied Adra2a antagonist [27-29]. In animals treated
170 with yohimbine, limbs contralateral to amputation had a significantly lower fraction of EdU+ cells
171 compared to vehicle-treated controls (Fig. 4b-c). Thus, we conclude that adrenergic signaling is required
172 for distant cell activation in response to amputation, and we propose this signal originates in the nerve.

173 Other candidate pathways we have tested include insulin and Wnt signaling. Our RNA-seq
174 dataset revealed that the expression of canonical Wnt signaling pathway transcription factor lymphoid
175 enhancer binding factor 1 (Lef1) is 5.9-fold increased in severed nerve ends. Intriguingly, Lef1 has
176 recently been shown to prime adult skin to enhance regeneration outcomes in mice [30] and is
177 expressed in the wound epidermis of regenerating zebrafish fins [31]. While Lef1 itself has not been
178 directly studied in the context of axolotl limb regeneration, Wnt signaling has been shown to regulate
179 limb regeneration in axolotl and *Xenopus* and fin regeneration in zebrafish [32]. Surprisingly, the
180 inhibition of Wnt signaling by the tankyrase inhibitor IWR-1 did not block systemic cell cycle re-entry
181 (Extended Data Fig. 6a-b), suggesting that the Wnt requirement may act locally, at the amputation site,
182 in axolotls. We also found transcripts encoding insulin-like growth factor 1 receptor (Igf1r) to be 19.2-
183 fold upregulated in tissues surrounding the nerve in denervated samples compared to sham-operated
184 controls. Igf1r is required for axonal regeneration of retinal ganglion cells from rats, and has been
185 implicated in progenitor activation mechanisms in several regeneration studies [33-35]. Inhibition of
186 Igf1r by an ATP-competitive inhibitor, NVP-ADW742 [35], blocked distant cell activation in limbs
187 contralateral to amputation, indicating that Igf-1 signaling is also required for this process (Extended
188 Data Fig. 6a-b). Taken together, our data suggest that nerve-mediated Adra2a signaling and Igf-1
189 signaling in the responding cells mediate systemic cell activation in response to amputation injury in
190 axolotl.

191 **Discussion**

192 Limb blastemas form at the site of amputation in salamanders, which has led the field to focus
193 on events occurring at the injury site. Early localized irradiation studies demonstrated that only cells
194 within the remaining limb stump are required to divide for regeneration [36]. While this lends support
195 to a model wherein only cells at the amputation site give rise to the blastema, understanding how cells
196 interpret injury signals in response to amputation is crucial to understanding regeneration. The
197 traditional view postulates that progenitor cells in the injured limb are activated upon amputation,
198 migrate to the tip of the stump, and proliferate to form the blastema. However, our earlier work
199 demonstrating that injury signals activate distant tissue progenitors [5] supports a model where cell
200 activation and blastema cell commitment are two separate events, and predicts that some activated
201 cells do not become blastema cells. This possibility led us to ask whether there could be an advantage to
202 having this system-wide activation that is later refined to the injury site. Here, we show that global
203 activation primes distant progenitors to respond faster in the event of an additional injury (Fig. 4d). This

204 “jump start” could serve as a selective advantage in salamanders, many species of which lay eggs in high
205 concentrations in small vernal pools [37], leading to dense aggregates of siblings and other conspecifics.
206 Salamanders developing in environments with limited space and resources are cannibalistic [38-41],
207 often resulting in amputation injuries to more than one limb in juveniles. Becoming poised for a future
208 injury upon losing a limb would allow the animal to quickly respond to subsequent loss of another limb,
209 and to produce new functional limbs, which is essential for their survival.

210 Our work provides mechanistic insights into how injury signals are transmitted to distant
211 locations. The nervous system has recently been implicated in mammalian systems in stem cell
212 mobilization [19, 20] and our work supports the idea that nerves can directly communicate with resident
213 progenitor cells to initiate cell cycle re-entry. Studies of other regeneration models have also implicated
214 circulation as a means to transduce injury signals [8, 13, 21]. While our work does not exclude the
215 possibility that factors circulating in the blood may also transmit injury signals, here we report a role of
216 nerves. Future work will help uncover whether similar signals are also carried through the blood in
217 axolotls. Our findings should prompt a re-evaluation of the role of peripheral nerves in the regenerative
218 process *per se*, including within the amputated limb itself, because it indicates a role for nerves in the
219 primary decision cells make to re-enter the cell cycle rather than simply serving to maintain proliferation
220 of cells that have independently made this choice.

221 Regeneration of complex body parts is often explained as an all-or-nothing phenomenon for a
222 given species. Yet, evidence that partial responses can occur, such as adult frogs regenerating
223 cartilaginous spikes missing many internal tissues and lacking appropriate patterning [42, 43], and lizards
224 regenerating tails lacking dorsal-ventral polarity and neuronal cell bodies [44-47], challenges this view.
225 Our data regarding systemic cellular activation in axolotl argues this feature may be a component of the
226 regenerative process and that it has a potentially selectable consequence of enhancing future
227 regenerative responses of distant tissues. Combined with previous reports of systemic activation
228 following injury in mice, we argue that a paradigm worth considering is that both species typically
229 classified as non-regenerators and as regenerators engage in a similar initial post-amputation response
230 that activates prospective progenitor cells throughout the body. This systemic response may therefore
231 be ancestral, present in mammals as a vestigial component of a broader regeneration program. In this
232 scenario, perhaps the key critical difference between the two types of animals is their ability to harness
233 this cellular activation at the site of injury, coalescing activated cells into a blastema, and sustaining
234 proliferation there long enough to spur regeneration. These issues have direct implications for
235 development of regenerative medicine approaches because a pool of proliferative progenitors is an
236 essential pre-requisite of coaxing a limb to regenerate without resorting to cellular transplantation. We
237 predict future therapies may harness endogenous stem cells that have been naturally and successfully
238 primed for appendage regeneration but require molecular instruction to transition to a blastema-like
239 state and, once instructed, these cells may organize a response more akin to salamander limb
240 regeneration.

241

242 **Methods**

243 **Animal Experimentation**

244 All animal experimentation was approved by and conducted in accordance with Harvard University's
245 Institutional Animal Care and Use Committee. Leucistic axolotls were used for all animal
246 experimentation except RNA sequencing and maintained as previously described [22]. For RNA
247 sequencing, *βIIItub:GAP43-EGFP* transgenic animals were used [48]. Animals in all experiments were
248 both age and size matched. Animals were anesthetized in 0.1% (w/v) tricaine prior to all procedures
249 involving amputation, denervation, or injection. After all surgical procedures, axolotls were allowed to
250 recover overnight in 0.5% (w/v) sulfamerazine. All limb amputations were performed at the mid-
251 stylopod and the bone was then trimmed back from the amputation plane. For forelimb denervations
252 the brachial plexus nerves were transected according to [49] and for hindlimb denervations the sciatic
253 nerves were transected according to [50]. Sham operations as controls for denervations were performed
254 by anesthetizing animals and cutting the skin open with sterile scissors, locating the nerve bundles with
255 closed sterile forceps, but not cutting the nerves.

256 **Drug treatments and EdU incorporation**

257 Rapamycin was dissolved into a 25 mg/ml stock solution in ethanol. Rapamycin treatments were
258 delivered via both water treatments at a concentration of 1 µM for 16 days with water changed daily,
259 and through daily intraperitoneal injections at a concentration of 5 mg/kg/day for 16 days, both starting
260 two days before amputation. All intraperitoneal injections were administered at a volume of 20µL/g in a
261 vehicle solution comprised of APBS with 5% Tween80, 5% PEG-400. All stock solutions were frozen at
262 −80 °C in 1-mL aliquots. Yohimbine (Y3125, Sigma-Aldrich) was dissolved into a 10 mg/mL stock solution
263 with sterilized water. Yohimbine was administered daily at a dose of 1mg/kg for 14 days via
264 intraperitoneal injection. A stock solution of IWR-1 (I0161, Sigma-Aldrich) was created by dissolving
265 5mg/mL in DMSO. IWR-1 was delivered daily at a dose of 10mg/kg/day for 9 days via intraperitoneal
266 injection. A stock solution of NVP-ADW742 (5247, Tocris) was created by dissolving 2mg/mL in DMSO.
267 NVP-ADW742 was injected daily at a dose of 10mg/kg/day for 14 days.

268 5-ethynyl-2'-deoxyuridine (EdU) was purchased from ThermoFisher and stock solutions were created by
269 dissolving the powder in dimethyl sulfoxide as instructed by the manufacturer. Following
270 anesthetization, axolotls were administered 20 µL/g of 400 µM EdU in 0.7X PBS via intraperitoneal
271 injection 18 hours before tissue harvest.

272 **Skeletal and tissue preparations**

273 For tissue sections, post-collection, tissue samples were fixed in 4% paraformaldehyde in DEPC-treated
274 PBS overnight at 4°C. Tissues were then cryopreserved in a sucrose gradient following a wash in DEPC-
275 PBS and incubated in 30% sucrose/DEPC-PBS at 4°C overnight. Tissues were then embedded and frozen
276 on dry ice in Tissue-Tek O.C.T. Compound (Sakura) and stored at −80°C. All blocks were sectioned at
277 16µm thickness using a Leica CM 1950 cryotome and sections were stored at −80°C until use.

278 For skeletal preparations, post-collection, limbs incubated overnight in 95% ethanol at room
279 temperature and then incubated in 100% acetone under the same conditions. Skeletal elements were
280 visualized with alcian blue and alizarin red S stains followed by a clearing of non-skeletal tissue with
281 potassium hydroxide.

282 **Immunofluorescence**

283 Sections were rehydrated with PBS and then permeabilized with 0.5% Triton-X-100 PBS. Post-
284 permeabilization, slides were rinsed twice with PBS and EdU visualization was performed via sulfo-
285 cyanine 3 azide (Lumiprobe). Post-EdU visualization slides were washed twice with PBS. Staining and
286 labeling with any additional antibodies was conducted post-EdU labeling. Primary antibodies used were
287 rabbit anti-phospho-S6 ribosomal protein (Ser235/236, 1:200; Cell Signaling 4858), mouse anti-NeuN
288 (1:200; Abcam ab104224), and rabbit anti-keratin 10 (BioLegend 905401). Secondary antibodies used
289 were Cy3-goat anti-mouse (1:250, Jackson ImmunoResearch 115-165-146), Alexa Fluor 488-Goat Anti-
290 Rabbit (1:250, Jackson ImmunoResearch, 111-545-003) and Cy3-goat anti-rabbit (1:250, Jackson
291 ImmunoResearch 111-165-003).

292 Sections stained with all antibodies were blocked with 10% serum from the host species of the
293 secondary antibody in 0.1% Triton-X-100 in PBS. Primary and secondary antibodies were diluted in in 2%
294 BSA, 0.1% Triton-X-100 in PBS. Sections labeled with anti-pS6 and NeuN underwent an antigen retrieval
295 step after permeabilization, in which slides were boiled in 0.1 M sodium citrate (pH 6.0) and then rinsed
296 once in PBS, before EdU was visualized, followed by blocking and primary antibody incubation. All slides
297 were incubated with DAPI (Sigma D9542) before cover slipping.

298 **Western blot**

299 Samples were harvested and blinded, protein extracted and western blots performed as in [22]. Primary
300 antibodies used were anti-pS6 (1:2000, Cell Signaling Technology 4858), anti-S6 (1:1000, Cell Signaling
301 Technology 2317S), and α-tubulin (1:2000, Sigma-Aldrich T9026); secondary antibodies used were goat
302 anti-rabbit HRP (1:5000, Jackson ImmunoResearch 111-035-003) and goat anti-mouse HRP (1:5000, Bio-
303 Rad 1721019).

304 **Imaging and quantification**

305 Imaging was performed on a Zeiss Axio Scan.Z1 automated slide scanner, Leica M165 FC equipped with
306 Leica DFC310 FX camera, and a Nikon Eclipse Ni microscope with a DS-Ri2 camera. Quantification of all
307 images was conducted blindly. For imaging of intact contralateral limbs, representative sections
308 displaying all tissue types (bone and cartilage, soft internal tissues, and epidermis) were selected. For
309 the tissue type analysis of EdU+ nuclei, tissues were classified as epidermis, “skeletal elements” (bone,
310 cartilage), and “soft tissues” (muscle, joint, tendon, ligaments, dermis, vasculature, and nerves) based
311 on nuclear morphology and location as previously described (Whited et al, 2013). All cell counts were
312 conducted utilizing CellProfiler [51]. Measurements of blastema area were performed using Fiji [52].

313 **Statistical analysis**

314 Statistical analysis of blastema differentiation was conducted using a Fisher’s exact test where $p < 0.05$
315 was considered to be significant. For statistical analysis of the number of digit outlines, a Chi-square test
316 comparing no digits, 2 digits and 3+ digits distribution between activated and control groups was utilized
317 in which $p \leq 0.05$ significant. Statistical analysis of the blastema area and length was performed using an
318 unpaired, two-tailed Welch’s t-test, with Holm-Šídák correction for multiple hypothesis testing, and an
319 adjusted p-value < 0.05 was considered significant.

320 For the quantification of %EdU+ nuclei in the limbs of animals in the denervation, long-chase EdU, and
321 inhibitor experiments the average of both the forelimb and hindlimb were taken and valued as a single
322 data point. Multiple unpaired, two-tailed Welch’s t-tests were used to analyze effect of mTOR inhibition

323 and denervation, with Bonferroni-Dunn correction for multiple hypothesis testing. For the remaining
324 experiments, a Welch's ANOVA was used to compare more than 2 groups, or an unpaired two-tailed
325 Welch's t-test, used to compare exactly two groups, were conducted assuming unequal variance. The
326 ANOVA was conducted under the parameters of post-hoc pairwise t-tests with Dunnett T3 correction for
327 multiple hypothesis testing. For all statistical analyses an adjusted-p-value < 0.05 was considered
328 significant.

329 **RNA isolation, sequencing, and computational analysis**

330 *βIIItub:GAP43-EGFP* transgenic animals were used for RNA sequencing experiments to allow for easily
331 identifiable collections of tissues [48]. RNA was extracted from tissue samples with Trizol (15596018,
332 Ambion) and chloroform (288306, Sigma Aldrich). RNA was then isolated from tissue samples using a
333 Zymo Clean Up and Concentrator kit (R1013). RNA samples were processed at the Bauer Core Facility at
334 Harvard University using the Illumina NextSeq 500. Paired End reads were demultiplexed with
335 bcl2fastq2 v2.2.

336 The reads were trimmed for quality and adapters with Trimmomatic v0.39 [53] with the following
337 parameters: LEADING:3 TRAILING:3 SLIDINGWINDOW:4:15 MINLEN:36. An index of the previously
338 published axolotl transcriptome [22] was created using Kallisto v0.45.1 [54]. Sequence based bias
339 correction was performed using Kallisto with 200 bootstraps across 20 threads. The transcript-level
340 abundances from Kallisto were summarized and imported into R as a matrix of counts using tximport
341 v1.0.3 [55].

342 Differentially expressed genes were determined by estimating fold change and dispersion using DESeq2
343 [56]. Genes were considered significant if they had a logarithmic fold change greater than 1.5 and
344 adjusted p value of 5%. These significant genes were visualized using pheatmap v1.0.12 [57]. Pathway
345 analysis was performed in R using pathfinder [58].

346 **Data availability**

347 The sequencing data associated with this study have been deposited in the Gene Expression Omnibus
348 (GEO) with the accession code GSE192477.

349

350 **References**

351

352 1. Ricci, L. and M. Srivastava, *Wound-induced cell proliferation during animal regeneration.* Wiley
353 Interdiscip Rev Dev Biol, 2018. **7**(5): p. e321.
354 2. Losner, J., K. Courtemanche, and J.L. Whited, *A cross-species analysis of systemic mediators of*
355 *repair and complex tissue regeneration.* NPJ Regen Med, 2021. **6**(1): p. 21.
356 3. Haas, B.J. and J.L. Whited, *Advances in Decoding Axolotl Limb Regeneration.* Trends Genet, 2017.
357 **33**(8): p. 553-565.
358 4. McCusker, C., S.V. Bryant, and D.M. Gardiner, *The axolotl limb blastema: cellular and molecular*
359 *mechanisms driving blastema formation and limb regeneration in tetrapods.* Regeneration (Oxf),
360 2015. **2**(2): p. 54-71.
361 5. Johnson, K., et al., *Systemic cell cycle activation is induced following complex tissue injury in*
362 *axolotl.* Dev Biol, 2018. **433**(2): p. 461-472.

363 6. Wenemoser, D. and P.W. Reddien, *Planarian regeneration involves distinct stem cell responses*
364 *to wounds and tissue absence.* Dev Biol, 2010. **344**(2): p. 979-91.
365 7. Srivastava, M., et al., *Whole-body acoel regeneration is controlled by Wnt and Bmp-Admp*
366 *signaling.* Curr Biol, 2014. **24**(10): p. 1107-13.
367 8. Rodgers, J.T., et al., *mTORC1 controls the adaptive transition of quiescent stem cells from G0 to*
368 *G(Alert).* Nature, 2014. **510**(7505): p. 393-6.
369 9. Maier, C.E. and M. Singer, *The effect of light on forelimb regeneration in the newt.* J Exp Zool,
370 1977. **202**(2): p. 241-4.
371 10. González-Estévez, C., et al., *SMG-1 and mTORC1 act antagonistically to regulate response to*
372 *injury and growth in planarians.* PLoS Genet, 2012. **8**(3): p. e1002619.
373 11. Tu, K.C., B.J. Pearson, and A. Sanchez Alvarado, *TORC1 is required to balance cell proliferation*
374 *and cell death in planarians.* Dev Biol, 2012. **365**(2): p. 458-69.
375 12. Hirose, K., et al., *Mechanistic target of rapamycin complex 1 signaling regulates cell*
376 *proliferation, cell survival, and differentiation in regenerating zebrafish fins.* BMC Dev Biol, 2014.
377 **14**: p. 42.
378 13. Haller, S., et al., *mTORC1 Activation during Repeated Regeneration Impairs Somatic Stem Cell*
379 *Maintenance.* Cell Stem Cell, 2017. **21**(6): p. 806-818 e5.
380 14. Molinaro, A.M., N. Lindsay-Mosher, and B.J. Pearson, *Identification of TOR-responsive slow-*
381 *cycling neoblasts in planarians.* EMBO Rep, 2021. **22**(3): p. e50292.
382 15. Gusel'nikova, V.V. and D.E. Korzhevskiy, *NeuN As a Neuronal Nuclear Antigen and Neuron*
383 *Differentiation Marker.* Acta Naturae, 2015. **7**(2): p. 42-7.
384 16. Todd, J.T., *On the process of reproduction of the members of the aquatic salamander.* . The
385 Quarterly Journal of Science, Literature, and the Arts. , 1823. **16**: p. 84-96.
386 17. Farkas, J.E. and J.R. Monaghan, *A brief history of the study of nerve dependent regeneration.*
387 Neurogenesis (Austin), 2017. **4**(1): p. e1302216.
388 18. Mahmoud, A.I., et al., *Nerves Regulate Cardiomyocyte Proliferation and Heart Regeneration.* Dev
389 Cell, 2015. **34**(4): p. 387-99.
390 19. Gao, X., et al., *Nociceptive nerves regulate haematopoietic stem cell mobilization.* Nature, 2021.
391 **589**(7843): p. 591-596.
392 20. Zhang, B., et al., *Hyperactivation of sympathetic nerves drives depletion of melanocyte stem*
393 *cells.* Nature, 2020. **577**(7792): p. 676-681.
394 21. Rodgers, J.T., et al., *HGFA Is an Injury-Regulated Systemic Factor that Induces the Transition of*
395 *Stem Cells into GAlert.* Cell Rep, 2017. **19**(3): p. 479-486.
396 22. Bryant, D.M., et al., *A Tissue-Mapped Axolotl De Novo Transcriptome Enables Identification of*
397 *Limb Regeneration Factors.* Cell Rep, 2017. **18**(3): p. 762-776.
398 23. Leigh, N.D., et al., *von Willebrand factor D and EGF domains is an evolutionarily conserved and*
399 *required feature of blastemas capable of multitissue appendage regeneration.* Evol Dev, 2020.
400 24. Kastan, N., et al., *Small-molecule inhibition of Lats kinases may promote Yap-dependent*
401 *proliferation in postmitotic mammalian tissues.* Nat Commun, 2021. **12**(1): p. 3100.
402 25. Chen, P., et al., *Dexmedetomidine promotes the progression of hepatocellular carcinoma*
403 *through hepatic stellate cell activation.* Exp Mol Med, 2020. **52**(7): p. 1062-1074.
404 26. Wang, W., X. Guo, and H. Dan, *alpha2A-Adrenergic Receptor Inhibits the Progression of Cervical*
405 *Cancer Through Blocking PI3K/AKT/mTOR Pathway.* Onco Targets Ther, 2020. **13**: p. 10535-
406 10546.
407 27. Blanchard, R.J., et al., *Yohimbine potentiates active defensive responses to threatening stimuli in*
408 *Swiss-Webster mice.* Pharmacol Biochem Behav, 1993. **44**(3): p. 673-81.
409 28. Ito, K., et al., *Endogenous alpha2A-Adrenoceptor-Operated Sympathoadrenergic Tones*
410 *Attenuate Insulin Secretion via cAMP/TRPM2 Signaling.* Diabetes, 2017. **66**(3): p. 699-709.

411 29. Mantsch, J.R., et al., *Involvement of noradrenergic neurotransmission in the stress- but not*
412 *cocaine-induced reinstatement of extinguished cocaine-induced conditioned place preference in*
413 *mice: role for beta-2 adrenergic receptors.* Neuropsychopharmacology, 2010. **35**(11): p. 2165-78.
414 30. Phan, Q.M., et al., *Lef1 expression in fibroblasts maintains developmental potential in adult skin*
415 *to regenerate wounds.* Elife, 2020. **9**.
416 31. Poss, K.D., J. Shen, and M.T. Keating, *Induction of lef1 during zebrafish fin regeneration.* Dev
417 Dyn, 2000. **219**(2): p. 282-6.
418 32. Kawakami, Y., et al., *Wnt/beta-catenin signaling regulates vertebrate limb regeneration.* Genes
419 Dev, 2006. **20**(23): p. 3232-7.
420 33. Tonkin, J., et al., *Monocyte/Macrophage-derived IGF-1 Orchestrates Murine Skeletal Muscle*
421 *Regeneration and Modulates Autocrine Polarization.* Mol Ther, 2015. **23**(7): p. 1189-1200.
422 34. Schertzer, J.D., et al., *Modulation of insulin-like growth factor (IGF)-I and IGF-binding protein*
423 *interactions enhances skeletal muscle regeneration and ameliorates the dystrophic pathology in*
424 *mdx mice.* Am J Pathol, 2007. **171**(4): p. 1180-8.
425 35. Mitsiades, C.S., et al., *Inhibition of the insulin-like growth factor receptor-1 tyrosine kinase*
426 *activity as a therapeutic strategy for multiple myeloma, other hematologic malignancies, and*
427 *solid tumors.* Cancer Cell, 2004. **5**(3): p. 221-30.
428 36. Butler, E.G., and O'Brien, J. P., *Effects of localized x-radiation on regeneration of the urodele*
429 *limb.* Anatomial Record, 1942. **84**(4): p. 407-413.
430 37. Rothenberger, M.B., Vera, M. K., Germanoski, D., Ramirez, E. , *Comparing amphibian habitat*
431 *quality and functional success among natural, restored, and created vernal pools.* Restoration
432 Ecology, 2019. **27**(4).
433 38. Pfennig, D.W. and J.P. Collins, *Kinship affects morphogenesis in cannibalistic salamanders.*
434 Nature, 1993. **362**(6423): p. 836-8.
435 39. Collins, J.P., Cheek, J. E. , *Effect of food and density on development of typical and cannibalistic*
436 *salamander larvae in Ambystoma tigrrinum nebulosum.* Ameican Zoologist, 1983. **23**: p. 77-84.
437 40. Thompson, S., et al., *Probability of Regenerating a Normal Limb After Bite Injury in the Mexican*
438 *Axolotl (Ambystoma mexicanum).* Regeneration (Oxf), 2014. **1**(3): p. 27-32.
439 41. Bothe, V., K. Mahlow, and N.B. Frobisch, *A histological study of normal and pathological limb*
440 *regeneration in the Mexican axolotl Ambystoma mexicanum.* J Exp Zool B Mol Dev Evol, 2021.
441 **336**(2): p. 116-128.
442 42. Dent, J.N., *Limb regeneration in larvae and metamorphosing individuals of the South African*
443 *clawed toad.* J Morphol, 1962. **110**: p. 61-77.
444 43. Yakushiji, N., H. Yokoyama, and K. Tamura, *Repatterning in amphibian limb regeneration: A*
445 *model for study of genetic and epigenetic control of organ regeneration.* Seminars in Cell &
446 Developmental Biology, 2009. **20**(5): p. 565-574.
447 44. Egar, M., S.B. Simpson, and M. Singer, *The growth and differentiation of the regenerating spinal*
448 *cord of the lizard, Anolis carolinensis.* J Morphol, 1970. **131**(2): p. 131-51.
449 45. Simpson, S.B., Jr., *Morphology of the regenerated spinal cord in the lizard, Anolis carolinensis.* J
450 Comp Neurol, 1968. **134**(2): p. 193-210.
451 46. Simpson, S.B., Jr., *Studies on regeneration of the lizard's tail.* Am Zool, 1970. **10**(2): p. 157-65.
452 47. Lozito, T.P. and R.S. Tuan, *Lizard tail skeletal regeneration combines aspects of fracture healing*
453 *and blastema-based regeneration.* Development, 2016. **143**(16): p. 2946-57.
454 48. Khattak, S., et al., *Germline transgenic methods for tracking cells and testing gene function*
455 *during regeneration in the axolotl.* Stem Cell Reports, 2013. **1**(1): p. 90-103.
456 49. Schotté, O.E. and E.G. Butler, *Morphological effects of denervation and amputation of limbs in*
457 *urodele larvae.* Journal of Experimental Zoology, 1941. **87**(2): p. 279-322.

50. Kropf, N., et al., *Sciatic nerve injury model in the axolotl: functional, electrophysiological, and radiographic outcomes.* J Neurosurg, 2010. **112**(4): p. 880-9.
51. McQuin, C., et al., *CellProfiler 3.0: Next-generation image processing for biology.* PLOS Biology, 2018. **16**(7): p. e2005970.
52. Schindelin, J., et al., *Fiji: an open-source platform for biological-image analysis.* Nature Methods, 2012. **9**(7): p. 676-682.
53. Bolger, A.M., M. Lohse, and B. Usadel, *Trimmomatic: a flexible trimmer for Illumina sequence data.* Bioinformatics, 2014. **30**(15): p. 2114-20.
54. Bray, N.L., et al., *Near-optimal probabilistic RNA-seq quantification.* Nat Biotechnol, 2016. **34**(5): p. 525-7.
55. Soneson, C., M.I. Love, and M.D. Robinson, *Differential analyses for RNA-seq: transcript-level estimates improve gene-level inferences.* F1000Res, 2015. **4**: p. 1521.
56. Love, M.I., W. Huber, and S. Anders, *Moderated estimation of fold change and dispersion for RNA-seq data with DESeq2.* Genome Biol, 2014. **15**(12): p. 550.
57. Kolde, R., *pheatmap: pretty heatmaps. R package version 1.0. 12. 2019*. 2019.
58. Ulgen, E., O. Ozisik, and O.U. Sezerman, *pathfindR: An R Package for Comprehensive Identification of Enriched Pathways in Omics Data Through Active Subnetworks.* Front Genet, 2019. **10**: p. 858.

Acknowledgements

This work was supported by The Richard and Susan Smith Family Odyssey Award (J.L.W.), the NIH New Innovator Award DP2HD087953 (J.L.W.) and Harvard University Faculty of Arts and Sciences (J.L.W.). We thank William Ye, Tyler Mourey, Kelly Dooling and Rui Qun Miao for animal care. We thank Matthew Warman, Marc Kirschner, Ya-Chieh Hsu, Davie Van Vactor, Rich Lee, Paul Garrity, and members of the Whited, Chiu, Greer and Lehoczky labs for discussions and comments on the manuscript. We thank Yulia Swartz for sharing reagents and assisting in data interpretation, Bobby Groves and Angelo Osofsky for technical assistance, and the Bauer Core Facility at Harvard University for sequencing.

Author Contributions

J.L.W., D.P.-D and S.E.W. conceived of the project. D.P.-D, S.E.W., B.E., S.H., J.L., J.V.M, and J.L.W. designed the experiments; D.P.-D. S.E.W., and J.L.W. wrote the paper; S.J.B. performed computational analyses; L.C. performed statistical analyses; D. P.-D., S.E.W., B.E., S.H., J.V.M., A.W., J.L., S.M and H.S. performed sample preparation, experiments, and experimental data analyses. All authors contributed to manuscript editing.

Competing Interests

J.L.W. is a co-founder of Matice Biosciences. Other authors declare no conflicts of interest.

Figures

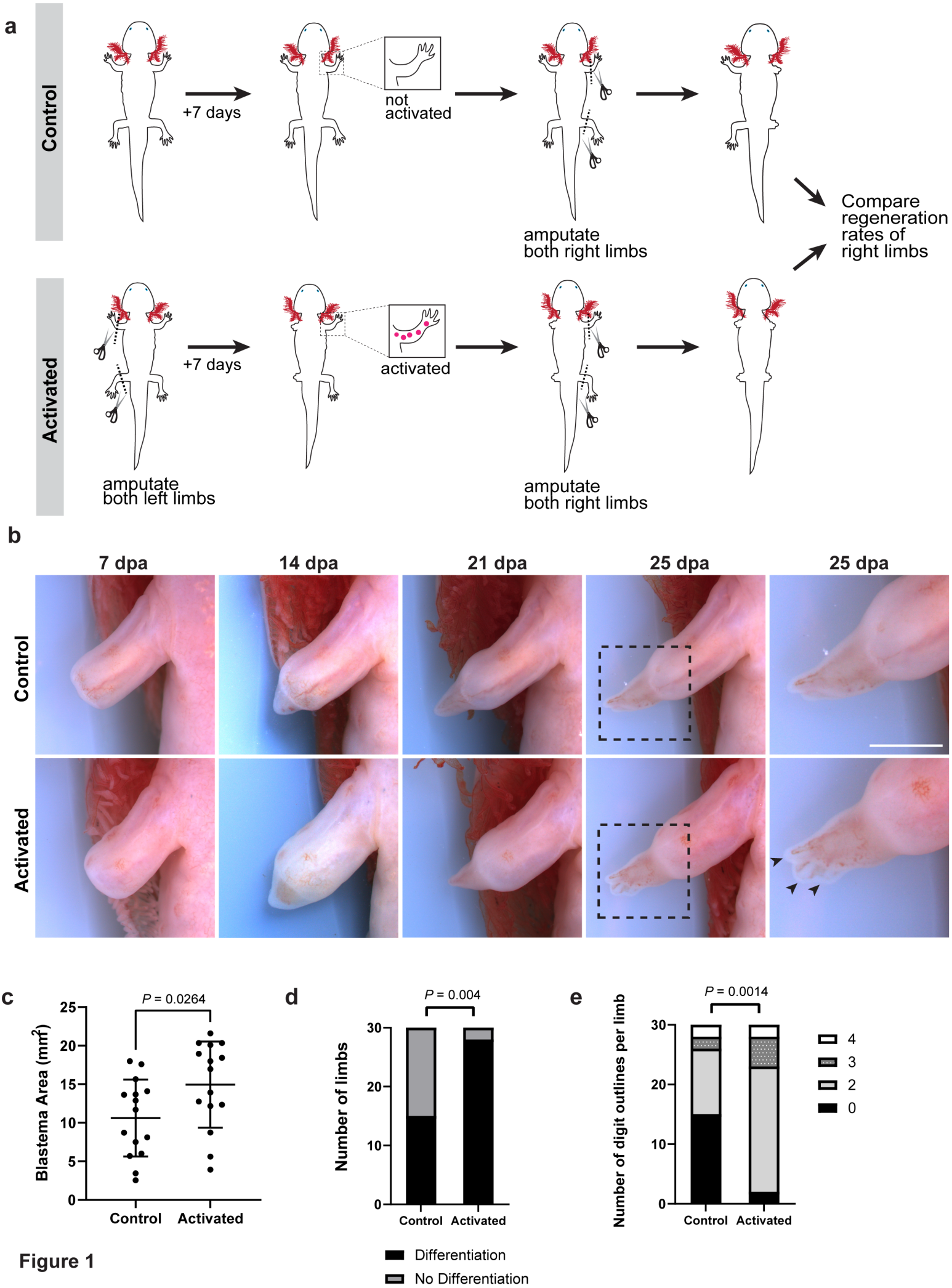
a
Control
+7 days
not activated
amputate both right limbs
Compare regeneration rates of right limbs
Activated
+7 days
activated
amputate both left limbs
amputate both right limbs
b
7 dpa
14 dpa
21 dpa
25 dpa
25 dpa
Control
Activated
c
P = 0.0264
Blastema Area (mm²)
Control
Activated
d
P = 0.004
Number of limbs
Control
Activated
e
P = 0.0014
Number of digit outlines per limb
Control
Activated
4
3
2
0
Differentiation
No Differentiation

Figure 1

502 **Figure 1. Systemically-activated cells are primed for future regeneration events.**
503 **a**, Experimental design. We compared regeneration rates of systemically-activated and naïve, control
504 limbs. Pink dots, activated, EdU positive nuclei. **b**, Representative images of regenerating systemically-
505 activated or control limbs. **c-e**, Quantification of blastema area at 14 days post-amputation **(c)**,
506 differentiating limbs **(d)**, and number of digit outlines **(e)** at 25 days post-amputation (n=15 animals for
507 each condition in blastema area measurement, analyzed by two-tailed Welch's t-test, n = 30 limbs for
508 each condition in differentiation and digit outline quantification, analyzed by Fisher's exact test for
509 differentiation and Chi-square test for digit outlines). All data shown as mean ± SD. Scale bars, 2 mm.
510 dpa, days post-amputation. EdU, 5-ethynyl-2'-deoxyuridine.
511

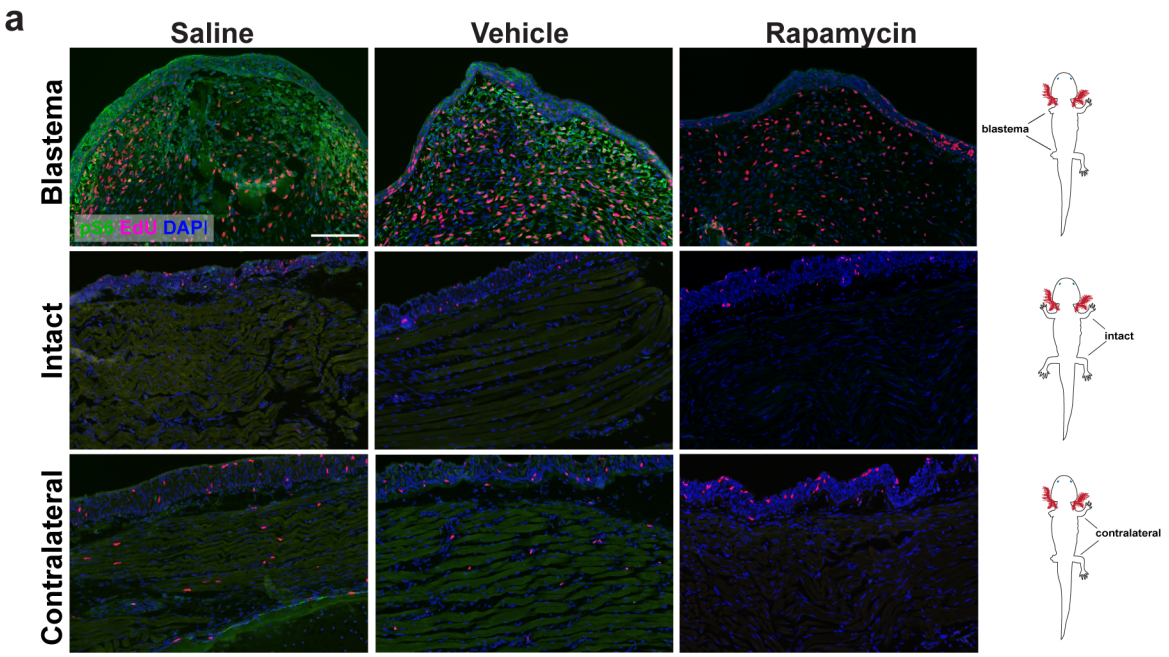
a
Saline
Vehicle
Rapamycin
Blastema
Intact
Contralateral
pS6 EdU DAPI
blastema
intact
contralateral
b
% EdU+ nuclei
P = 0.0152
P = 0.0029
P > 0.9999
saline int
saline contra
vehicle int
vehicle contra
rapa int
rapa contra

Figure 2

512 **Figure 2. mTOR signaling is required for systemic activation. a**, pS6 and EdU staining of blastema, intact
513 (homeostatic) and contralateral limb tissue sections from animals treated with saline, vehicle, or
514 rapamycin at 14 dpa. **b**, Quantification of EdU positive nuclei at 14 dpa. (n = 12 limbs for intact saline,
515 intact vehicle and intact rapamycin groups, n = 10 limbs for amputated saline and amputated vehicle,
516 and n = 8 limbs for amputated rapamycin groups, analyzed by unpaired two-tailed Welch's t-tests with
517 Bonferroni-Dunn correction). All data shown as mean ± SD. Scale bar, 500 µm. rapa, rapamycin. Int,
518 intact. contra, contralateral. dpa, days post-amputation. pS6**,** phospho-S6 ribosomal protein; EdU, 5-
519 ethynyl-2'-deoxyuridine.

520

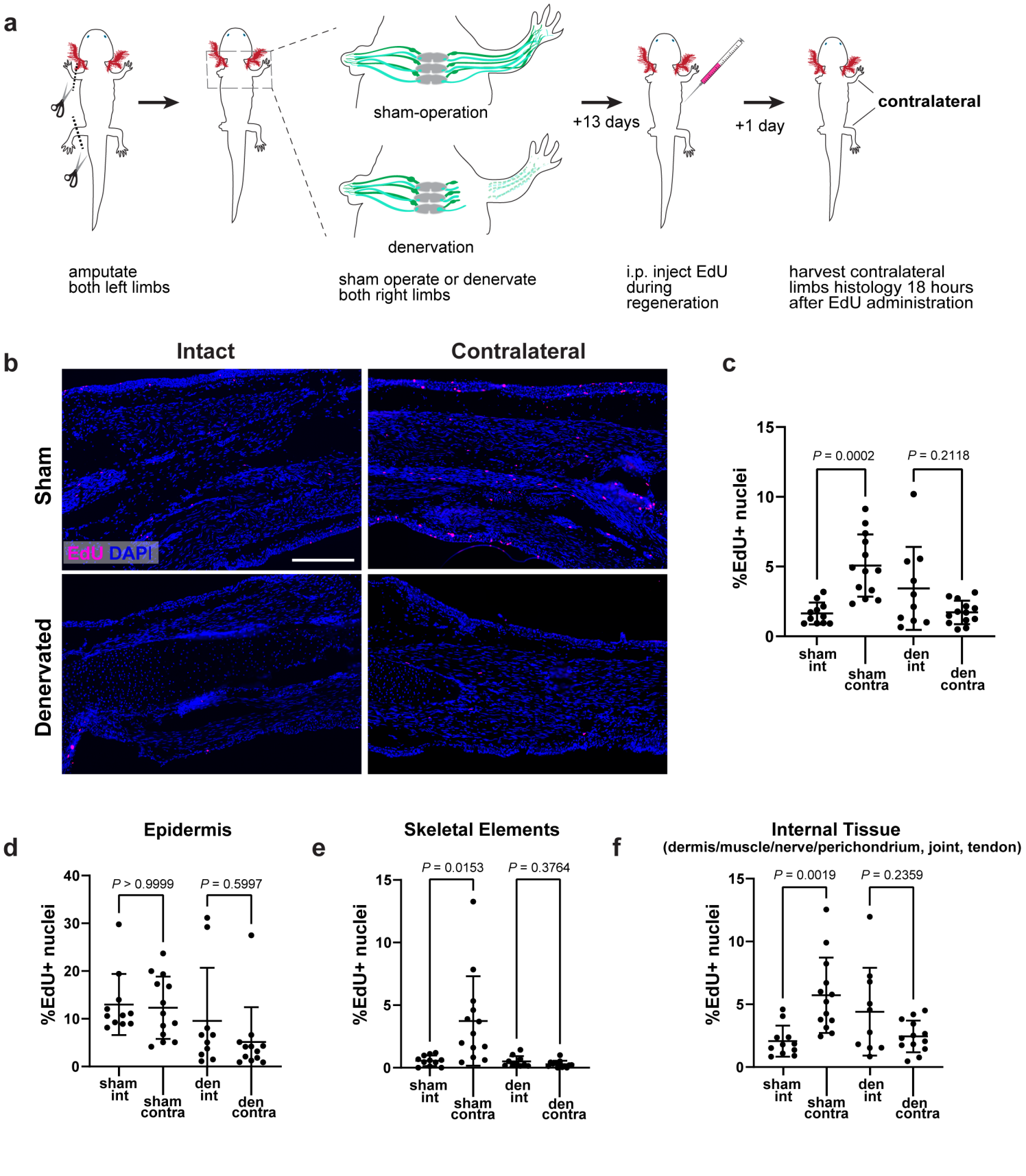
a
sham-operation
denervation
+13 days
+1 day
contralateral
amputate
both left limbs
sham operate or denervate
both right limbs
i.p. inject EdU
during
regeneration
harvest contralateral
limbs histology 18 hours
after EdU administration
b
Intact
Contralateral
Sham
Denervated
EdU DAPI
c
%EdU+ nuclei
P = 0.0002
P = 0.2118
sham int
sham contra
den int
den contra
d
Epidermis
P > 0.9999
P = 0.5997
e
Skeletal Elements
P = 0.0153
P = 0.3764
f
Internal Tissue
(dermis/muscle/nerve/perichondrium, joint, tendon)
P = 0.0019
P = 0.2359

Figure 3

521 **Figure 3. Nerves are required for systemic activation. a**, Experimental design. Nerve bundles
522 innervating limbs contralateral to unilateral amputations were transected or sham-operated, and
523 animals were assayed for systemic activation. Animals receiving unilateral denervations or sham-
524 operations with no amputations were used as controls. **b**, EdU and DAPI staining of intact and
525 contralateral limb tissue sections of denervated and sham-operated animals in the intact state or at 14
526 days post amputation. **c-f**, Quantification of percent EdU positive nuclei in denervated and sham-
527 operated limbs **(c)**, epidermis **(d)**, skeletal elements **(e)**, and soft internal tissues **(f)** at 14 dpa. (n = 11
528 animals for sham, n = 10 animals for denervated, n = 13 animals for sham amputated and denervated
529 amputated, analyzed by unpaired two-tailed Welch's t-tests with Bonferroni-Dunn correction). All data
530 shown as mean ± SD. Scale bar, 500 µm. den, denervated. int, intact. contra, contralateral. EdU, 5-
531 ethynyl-2'-deoxyuridine.
532

a

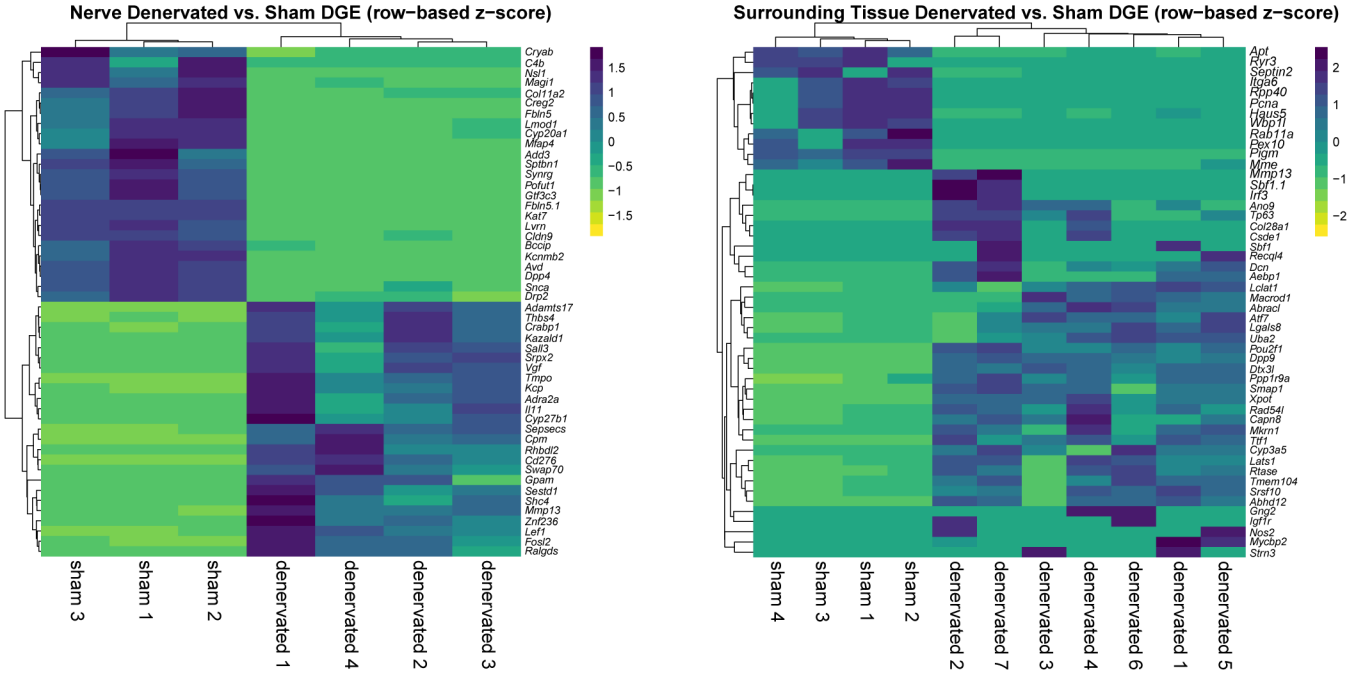

b

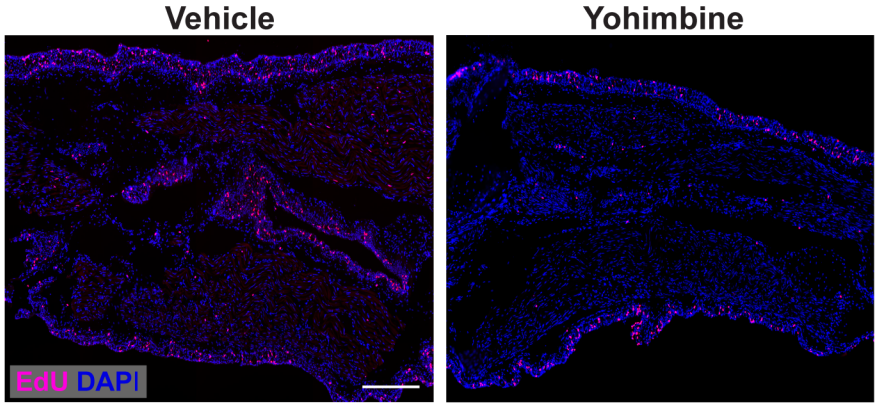

c

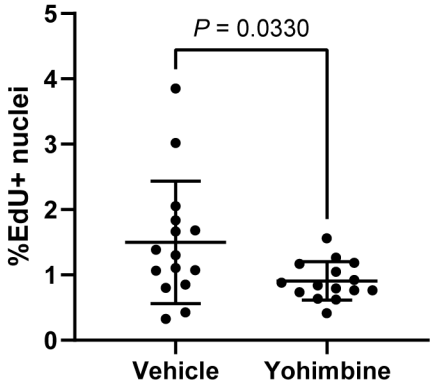

d

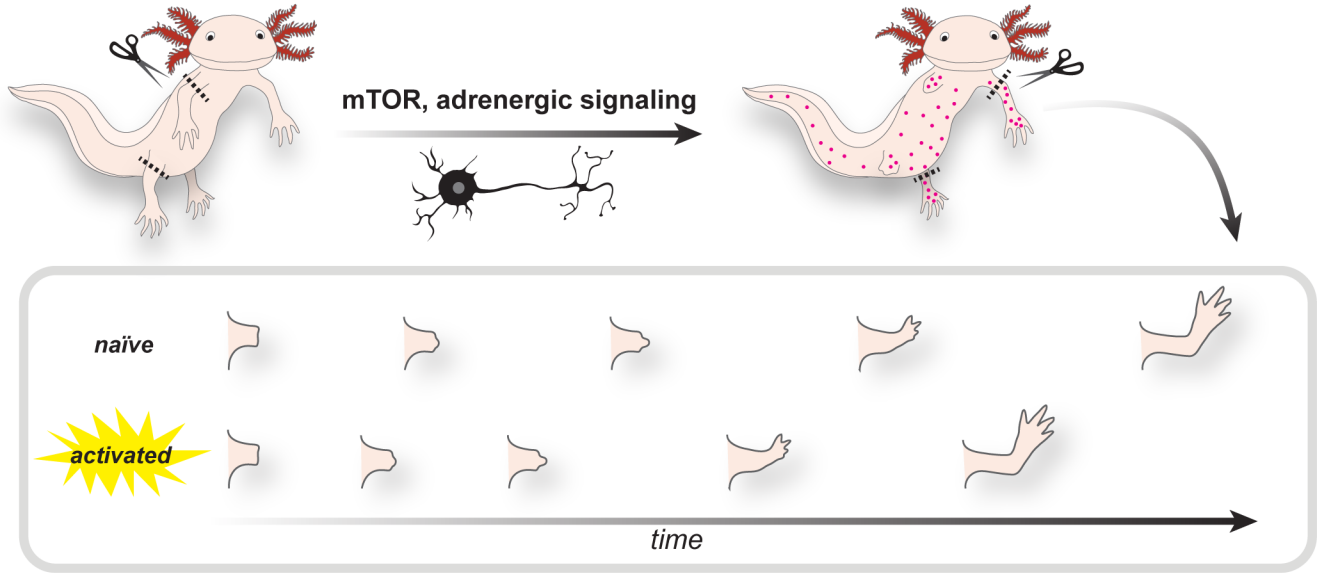

Figure 4

533 **Figure 4. Transcriptome analyses reveal pathways regulating systemic activation.** Nerves servicing
534 limbs contralateral to unilateral amputations were transected or sham-operated. Nerve ends and the
535 immediate tissue surrounding them were collected 14 days post amputation. **a**, Differential gene
536 expression analysis identifies transcripts that are enriched in nerve ends (left) and responding tissues
537 (right). **b**, EdU and DAPI staining of limbs contralateral to unilateral amputations treated with yohimbine
538 or vehicle control, harvested at 7 days post amputation. **c**, Quantification of percent EdU positive nuclei
539 in contralateral limbs in **(b)** (n = 15 animals for each group, analyzed by unpaired two-tailed Welch's t-
540 test). All data shown as mean ± SD. Scale bar, 500 µm. EdU, 5-ethynyl-2'-deoxyuridine. **d**, Model
541 summarizing the main findings of the study. Limbs activated by a prior contralateral amputation
542 regenerate faster than naïve, control limbs. This effect is mediated by nerves, mTOR signaling, and
543 adrenergic signaling.

544

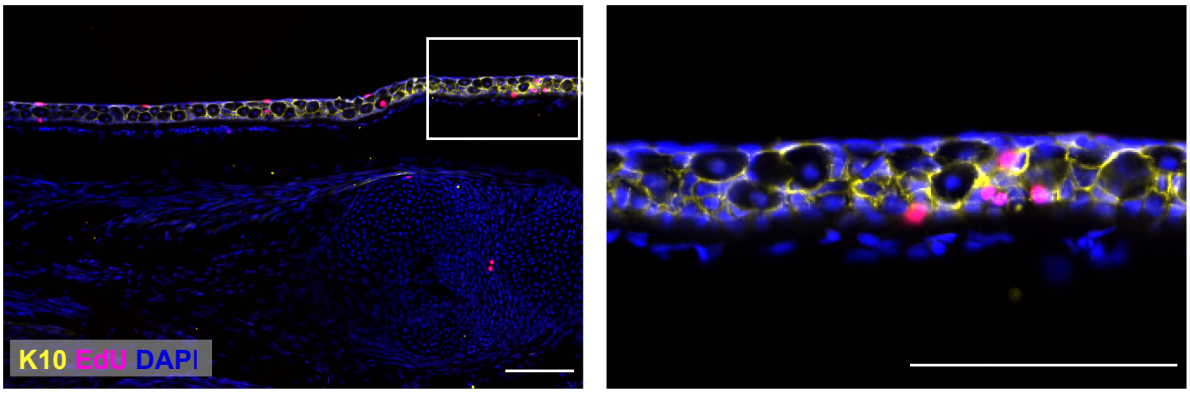

Extended Data Figure 1

545 **Extended Data Figure 1. A subset of activated cells are epidermal stem cells.** Keratin 10, EdU and DAPI
546 staining of limbs contralateral to amputation harvested 14 days post amputation, 18 hours after EdU
547 administration**.** Data shown as mean ± SD. Scale bars, 200 µm. K10, keratin 10. EdU, 5-ethynyl-2'-
548 deoxyuridine.
549
550

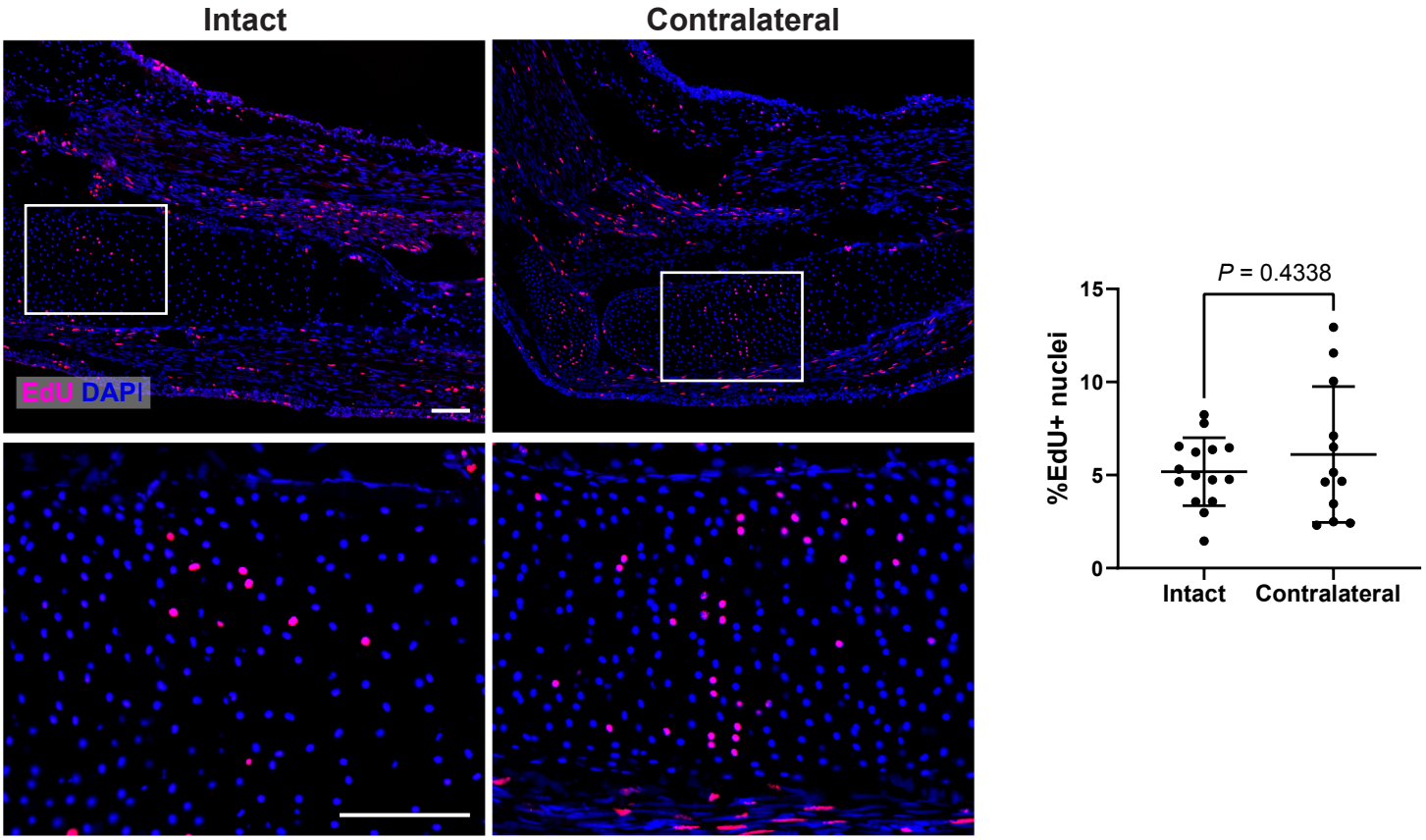

Extended Data Figure 2

551 **Extended Data Figure 2. Activated cells in distant limbs form clones. a,** EdU and DAPI staining of intact
552 limbs (left) and limbs contralateral to amputation (right) harvested 6 weeks after EdU administration. **b,**
553 Quantification of percent EdU positive nuclei of intact and contralateral limbs. (n = 15 animals for intact
554 and n = 12 animals for contralateral group, analyzed by unpaired two-tailed Welch's t-test). Data shown
555 as mean ± SD. Scale bar, 500 µm. EdU, 5-ethynyl-2'-deoxyuridine.
556

557

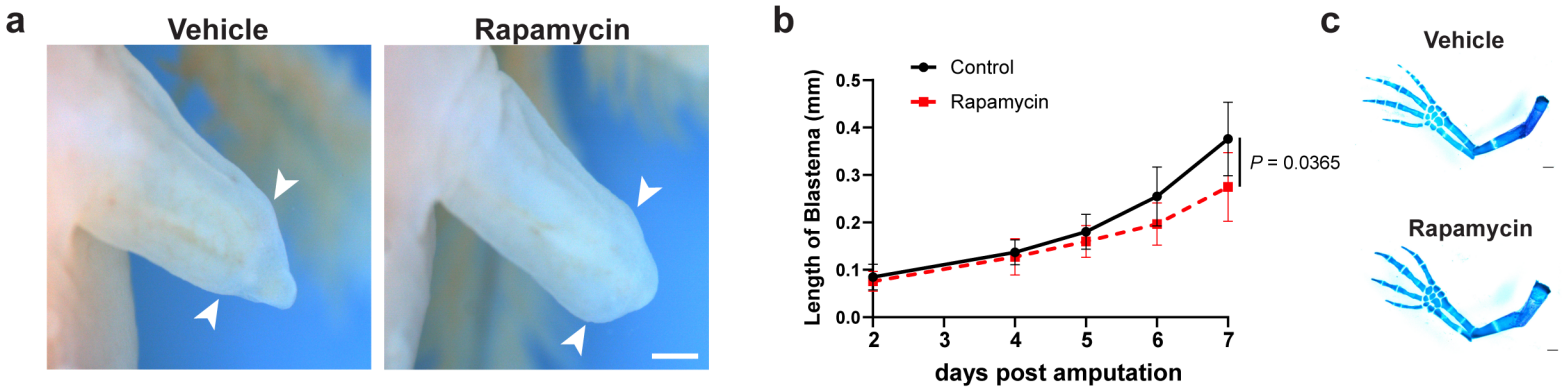

Extended Data Figure 3

558 **Extended Data Figure 3. Rapamycin-treated animals produce smaller blastemas.**
559 **a**, Regenerating limbs at 7 dpa treated with rapamycin or vehicle control. Arrowheads mark the
560 amputation plane. **b**, Blastema growth curves of rapamycin or vehicle treated animals. (n = 10 animals
561 per group, analyzed by unpaired two-tailed Welch's t-test with Holm-Šídák correction). **c**,
562 Representative skeletal preparations of regenerated limbs with Alcian blue and Alizarin red at 10 weeks
563 post amputation. Scale bars, 0.5 mm.
564

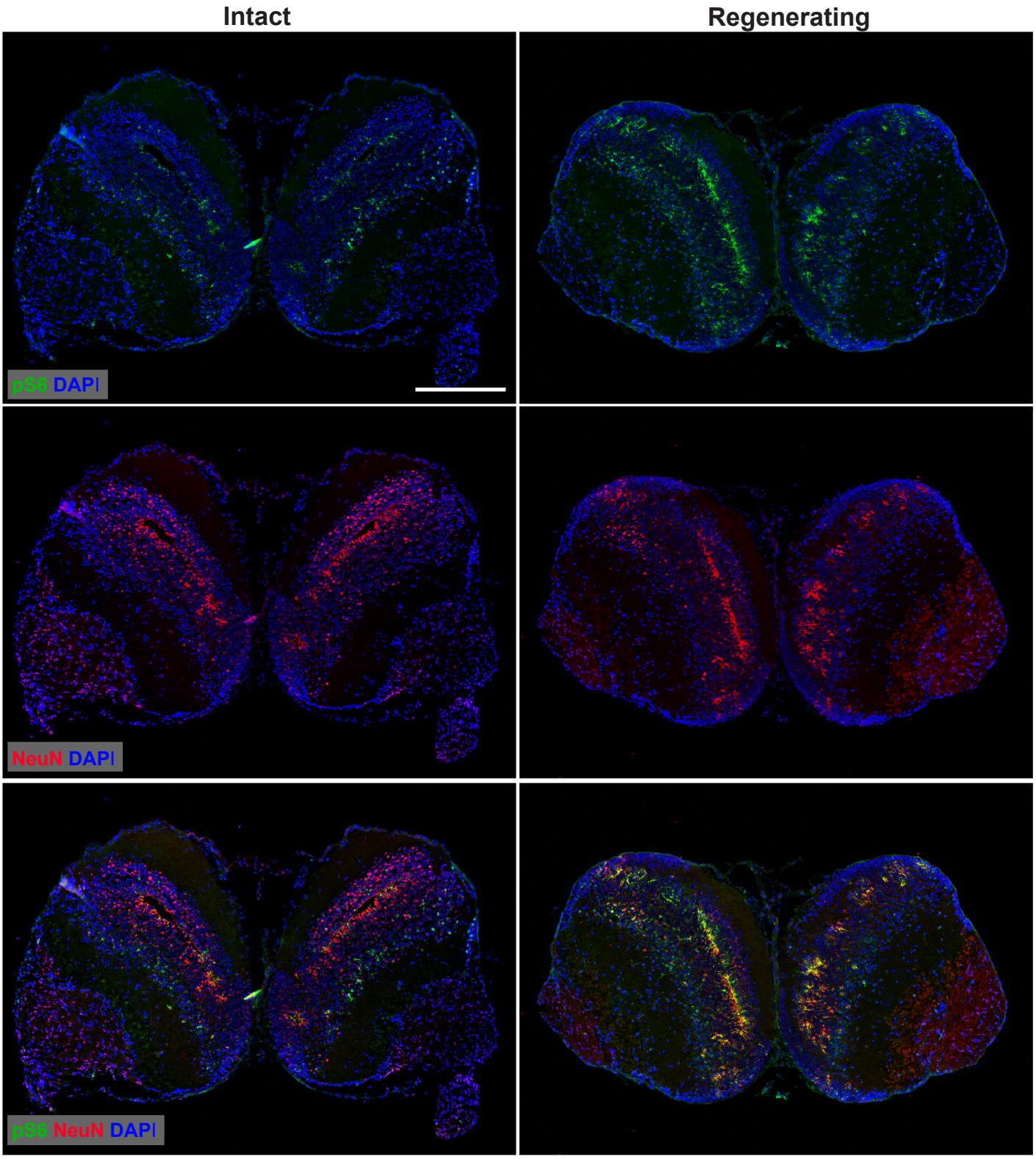

Extended Data Figure 4

565 **Extended Data Figure 4. mTOR signaling is upregulated in the brains of animals with regenerating**
566 **limbs.** pS6 and NeuN staining of anterior telencephalon sections of animals with intact (left) or
567 regenerating (right) limbs harvested at 7 days post amputation. Scale bar, 200 µm. pS6**,** phospho-S6
568 ribosomal protein. NeuN, neuronal nuclear protein.

569

a

same animal

Intact | Regenerating | Contralateral

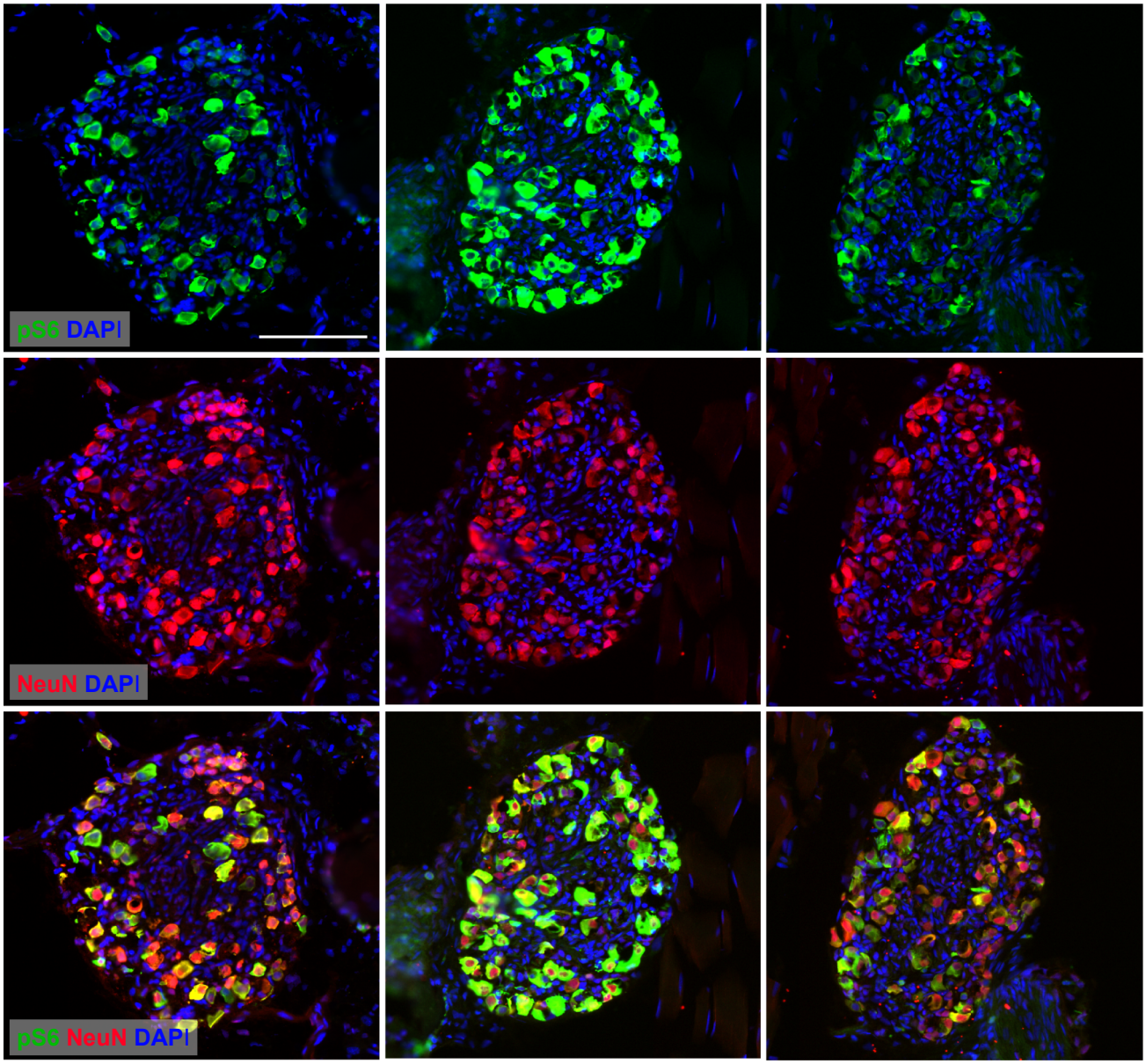

b

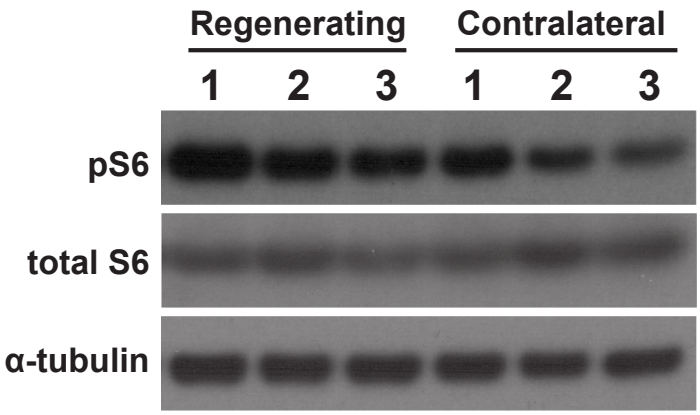

Extended Data Figure 5

570 **Extended Data Figure 5. mTOR signaling is differentially regulated in the dorsal root ganglia of sensory**
571 **nerves innervating the regenerating limb. a**, pS6 and NeuN staining of dorsal root ganglia servicing
572 intact, regenerating, and contralateral limbs at 7 days post amputation. **b**, Western blot of pS6 and total
573 S6 protein levels in dorsal root ganglia servicing regenerating and contralateral limbs harvested at 3 days
574 post amputation. Alpha-tubulin serves as loading control. Lanes with same numbers correspond to
575 dorsal root ganglia harvested from the same animal. Scale bar, 200 µm. pS6**,** phospho-S6 ribosomal
576 protein. NeuN, neuronal nuclear protein.

577

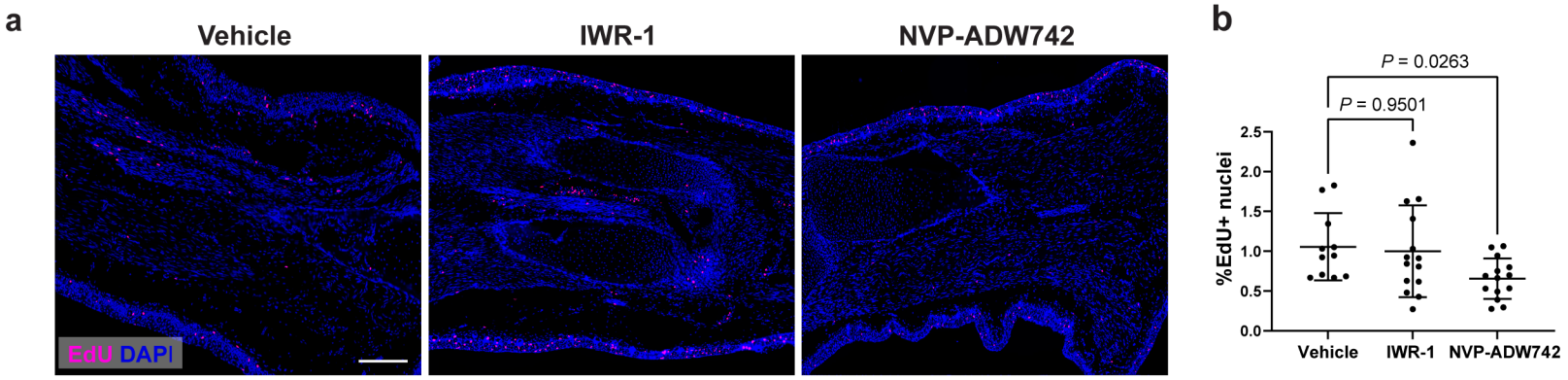

Extended Data Figure 6

578 **Extended Data Figure 6. Test of additional candidate pathways regulating systemic activation. a**, EdU
579 and DAPI staining of limbs contralateral to unilateral amputations treated with tankyrase inhibitor IWR-
580 1, Igf1r inhibitor NVP-ADW742 or vehicle control, harvested at 7 days post amputation. **b,** Quantification
581 of percent EdU positive nuclei of contralateral limbs in **(a)**. (n = 11 animals for vehicle control, n = 14
582 animals for IWR-1 and NVP-ADW742, analyzed by Welch's ANOVA with Dunnett's T3 correction, W =
583 4.883). All data shown as mean ± SD. Scale bar, 500 µm. EdU, 5-ethynyl-2'-deoxyuridine.

584

585